PROCEEDINGS OF THE INTERNATIONAL CONFERENCE
NANOMATERIALS: APPLICATIONS AND PROPERTIES
Vol. **3** No 2, 02NAESF03(3pp) (2014)

THz Emission from Dipolariton Systems

I.A. Shelykh[1,2,*], O. Kyriienko[1,2], K. Kristinsson[1], T.C.H. Liew[1]

[1] *Division of Physics and Applied Physics, Nanyang Technological University 637371 Singapore*
[2] *Science Institute, University of Iceland, Dunhagi-3, IS-107, Reykjavik, Iceland*

(Received 07 March 2014; published online 29 August 2014)

Dipolaritons are mixed light-matter quasiparticles formed in double quantum wells embedded in microcavities. Resonant excitation of the cavity mode can induce oscillations of the indirect exciton density with a characteristic frequency of Rabi flopping. This results in oscillations of classical Hertz dipoles, which generate superradiant emission with terahertz (THz) frequency. Both regimes of pulsed and continuous emission can be realized. The resulting THz signal may be sufficiently enhanced using a supplementary THz cavity tuned in resonance with the oscillation frequency.

Keywords: Dipolariton, THz emitter, Superradiance, Exciton, Polariton.

PACS numbers: 71.36. + c, 78.67.Pt, 42.65. – k, 71.35. – y

1. INTRODUCTION

Theoretical proposals for THz sources in semiconductor physics present a rich diversity. One of the classes of solid state THz emitters is represented by polariton-based devices, where signals are generated from transitions between upper and lower polariton branches [1], transitions between 2*p* exciton and 1*s* exciton-polariton states [2], or bosonic cascade lasers [3]. The proposal we consider here is based on the recent experimental realization of dipolaritons — cavity exciton-polaritons characterized by large dipole moments [4].

The described mechanism for terahertz signal generation relies on the beats between spatially direct and indirect excitons. Spatially indirect excitons are composed of electrons and holes situated in separate quantum wells (QWs). Recently, it has been shown that exciton-polaritons and spatially indirect excitons can be intermixed in biased semiconductor microcavities with embedded coupled QWs [4]. In these structures new quasiparticles being linear superpositions of cavity photon (C), direct exciton (DX) and indirect exciton (IX) modes appear. They form three exciton-polariton modes, namely, the upper polariton (UP), middle polariton (MP) and lower polariton (LP) modes. These modes may be characterized by large dipole moments, which is why they are referred to as *dipolaritons* [4].

The combination of the tunneling and cavity-exciton coupling can result in Rabi flopping between the dipolariton modes and lead to harmonic oscillations of IX density. Since indirect excitons represent elementary dipoles, these density oscillations result in emission of THz frequency radiation whose characteristics can be tuned by the applied bias and pumping conditions. This mechanism of THz radiation is similar to downshift optical-to-THz frequency conversion used in laser driven terahertz emitters. The essential difference of the generation scheme we propose from the previously studied schemes is in the use of the superradiance effect appearing due to the fact that Rabi oscillations in the dipolariton system are coherent.

We consider theoretically three cases. First, we consider the Rabi oscillations in the regime of pulsed excitation, which can result in the strong outburst of THz radiation on the duration of several tens of picoseconds [5]. Second, we show that strong exciton-exciton interactions can lead to the appearance of parametric instability and Hopf bifurcation in the system in the regime of CW pump, which leads to the possibility of continuous THz emission [6]. Finally, we consider the system embedded inside a THz cavity tuned in resonance with the THz Rabi frequency and investigate the onset of THz lasing in the system [7].

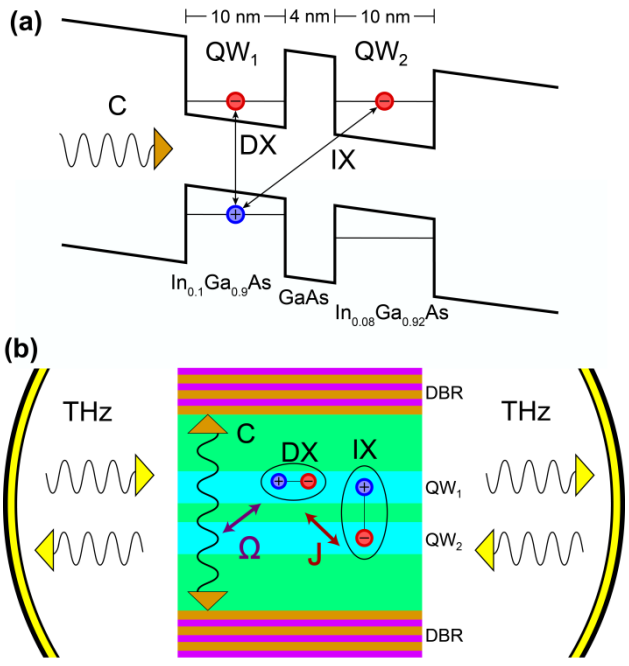

Fig. 1 – (a) Band diagram of the double QW system. In the presence of the optical microcavity the QW_1 is coupled to the cavity mode. The energy bands are tilted by the applied electric field, bringing the electron levels into resonance. Dimensions and materials of the QWs and the barrier are indicated. (b)

* ishelykh@ntu.edu.sg

Sketch of the dipolariton system in a THz cavity. The QW_1 is where direct excitons (DX) are excited. The electron can tunnel with a rate J to the QW_2, forming indirect excitons (IX). The distributed Bragg reflectors (DBR) provide the confinement of the cavity photon (C), which is strongly coupled to the direct exciton transition with a Rabi frequency Ω, and decoupled from the QW_2. The supplemental cavity hosts a THz photonic mode, which interacts with the exciton dipole moment

2. GEOMETRY OF THE SYSTEM AND EQUATIONS OF MOTION

In the most general case, the geometry of the considered structure is shown in Figure 1. It contains a double QW system hosting direct and indirect excitons coupled by resonant tunneling, embedded within an optical cavity tuned in resonance with the direct exciton optical transition and, possibly, into an additional THz cavity.

The Hamiltonian of the system written in the second quantization representation reads [7]:

$$\hat{H} = \hat{H}_0 + \hat{H}_{int} + \hat{H}_{nonl} + P(t)\hat{a}_c^\dagger + P(t)^*\hat{a}_c, \qquad (1)$$

where the first term is

$$\hat{H}_0 = \hbar\omega_T\hat{a}^\dagger\hat{a} + \hbar\omega_D\hat{b}^\dagger\hat{b} + \hbar\omega_I\hat{c}^\dagger\hat{c} + \hbar\omega_c\hat{a}_c^\dagger\hat{a}_c + \\ + \tfrac{1}{2}\hbar\Omega\left(\hat{a}_c^\dagger\hat{b} + \hat{b}^\dagger\hat{a}_c\right) - \tfrac{1}{2}\hbar J(\hat{b}^\dagger\hat{c} + \hat{c}^\dagger\hat{b}), \qquad (2)$$

and describes the energy of the free mode terms of the THz mode ($\hbar\omega_T$), the direct exciton ($\hbar\omega_D$), the indirect exciton ($\hbar\omega_I$) and optical cavity mode ($\hbar\omega_c$), as well as the DX-IX tunneling with rate J and direct exciton to optical photon coupling Ω.

The second term corresponds to the emission of THz photons and can be represented as

$$\hat{H}_{int} = -\left[g\hat{c}^\dagger\hat{c} + \tilde{g}\left(\hat{b}^\dagger\hat{c} + \hat{c}^\dagger\hat{b}\right)\right]\left(\hat{a} + \hat{a}^\dagger\right), \qquad (3)$$

where $g = eL\sqrt{\hbar\omega_T/2\epsilon V}$ and $\tilde{g} \approx 0.17g$ [7] are the exciton-THz photon coupling constants.

The third term, corresponding to nonlinear processes, is given by

$$\hat{H}_{nonl} = \tfrac{\alpha_1}{2}\hat{b}^\dagger\hat{b}^\dagger\hat{b}\hat{b} + \tfrac{\alpha_3}{2}\hat{c}^\dagger\hat{c}^\dagger\hat{c}\hat{c} + \alpha_2\hat{b}^\dagger\hat{c}^\dagger\hat{b}\hat{c}. \qquad (4)$$

It describes the Coulomb scattering of two direct excitons with interaction constant α_1, two indirect excitons with constant α_3, and the interspecies scattering of a direct and an indirect exciton with constant α_2. The estimation of these constants can be found in Ref. [6].

The last term corresponds to the coherent pump of the optical cavity mode, which can be chosen either CW or pulsed.

The corresponding equations for classical amplitudes of the fields in the mean field approximation read:

$$\frac{\partial}{\partial t}\langle\hat{a}\rangle = -i\omega_T\langle\hat{a}\rangle + i\tfrac{g}{\hbar}|\langle\hat{c}\rangle|^2 + i\tfrac{2\tilde{g}}{\hbar}\mathrm{Re}\left[\langle\hat{b}\rangle^*\langle\hat{c}\rangle\right] - \tfrac{1}{2\tau_T}\langle\hat{a}\rangle, \qquad (5)$$

$$\frac{\partial}{\partial t}\langle\hat{a}_c\rangle = -\tfrac{i}{2}\Omega\langle\hat{b}\rangle - \tfrac{1}{2\tau_C}\langle\hat{a}_c\rangle - i\tilde{P}(t), \qquad (6)$$

$$\frac{\partial}{\partial t}\langle\hat{b}\rangle = i\delta_\Omega\langle\hat{b}\rangle - \tfrac{i}{2}\Omega\langle\hat{a}_c\rangle + \tfrac{i}{2}J\langle\hat{c}\rangle + i\tfrac{2\tilde{g}}{\hbar}\mathrm{Re}[\langle\hat{a}\rangle]\langle\hat{c}\rangle \\ - \tfrac{i}{\hbar}\left(\alpha_1|\langle\hat{b}\rangle|^2 + \alpha_2|\langle\hat{c}\rangle|^2\right)\langle\hat{b}\rangle - \tfrac{1}{2\tau_{DX}}\langle\hat{b}\rangle, \qquad (7)$$

$$\frac{\partial}{\partial t}\langle\hat{c}\rangle = i(\delta_\Omega - \delta_J)\langle\hat{c}\rangle + \tfrac{i}{2}J\langle\hat{b}\rangle + i\tfrac{2}{\hbar}\mathrm{Re}[\langle\hat{a}\rangle]\left(g\langle\hat{c}\rangle + \tilde{g}\langle\hat{b}\rangle\right) \\ - \tfrac{i}{\hbar}\left(\alpha_2|\langle\hat{b}\rangle|^2 + \alpha_3|\langle\hat{c}\rangle|^2\right)\langle\hat{c}\rangle - \tfrac{1}{2\tau_{IX}}\langle\hat{c}\rangle, \qquad (8)$$

where $\delta_J = \omega_I - \omega_D$, $\delta_\Omega = \omega_c - \omega_D$, and we introduced phenomenologically the lifetimes of the modes. The detuning between direct and indirect excitons δ_J can be efficiently controlled by the voltage applied perpendicular to the structure interface.

If one considers the regime when the THz cavity is absent and thus THz photons are supposed to leave the system immediately, one should set $\langle\hat{a}\rangle = 0$ in the above equations.

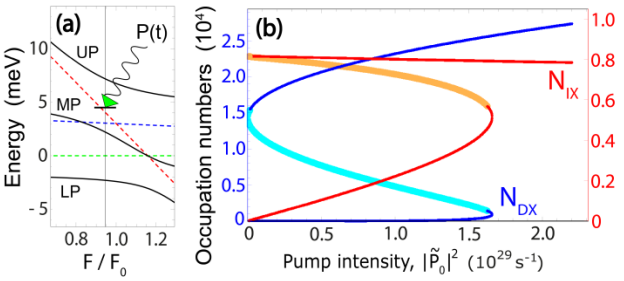

Fig. 2 – (a) Energy diagram of the dipolariton system, as a function of the applied field F in units of the resonance field F_0. The dashed lines correspond to the bare modes, the photonic (green and flat), the DX (blue) and the IX (red and steep) modes. The diagonalized modes, being the upper (UP), middle (MP) and lower (LP) dipolaritons, are indicated with solid lines. The energy of the pump is identified with a short horizontal line. The vertical line shows the value of the applied field chosen for the calculations. (b) Stability curve under CW pumping for pumping energy $\hbar\Delta_p = \hbar(\omega - \omega_c) = 4.5$ meV. The bistability arises here due to the blueshift of the MP mode. The blue curve indicates the DX numbers (left axis), and the red curve the IX numbers (right axis). Thin segments indicate stability of the population numbers, while the thick lines indicate parametric instability.

3. DISCUSSION

The system of equations (5)-(8) can be analyzed numerically for various regimes of pumping strength given by the term $P(t)$.

For pulsed pumping the photons introduced initially into the cavity mode are transferred coherently into direct excitons due to the Rabi coupling and then into indirect excitons due to the resonant tunneling of the electrons between QWs. The system thus enters into the regime of Rabi oscillations between the modes associated with alternations of the total dipole moment, thus providing THz emission. These oscillations, however, are decaying due to the finite lifetime of the modes, and thus emission occurs only during a finite interval of time (tens of picoseconds for realistic parameters).

In order to obtain a continuous THz emission one needs to compensate the finite lifetime of the modes and thus use a CW pump, taking the pumping term in Eq. (6) as $\tilde{P}(t) = P_0 e^{-i\omega t}$ with ω being the pumping energy. Note, however, that in this case one can at the end achieve the stationary values of the population of the modes with no THZ emission, for which the oscillatory behavior of the dipole moment is necessary. This situation is realized for small values of pumping intensities, where the role of nonlinearities provided by exciton-exciton interactions is negligible. However, after passing some threshold the Hopf bifurcation occurs, the stationary solution loses its stability, and continuous THz emission becomes possible [6].

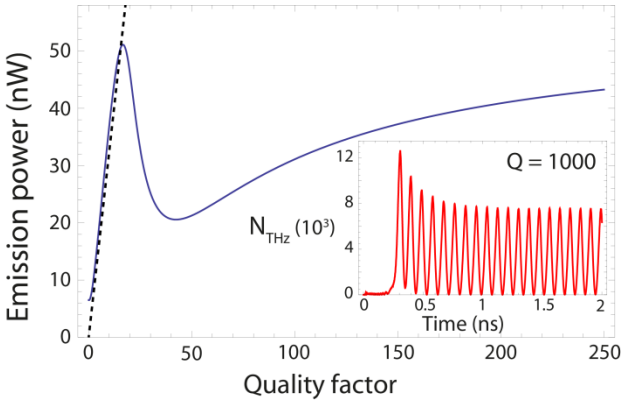

Fig. 3 – Plot of the time averaged emission power of THz radiation as a function of the quality factor of the THz cavity. The dashed line shows the low Q Purcell effect approximation. A peak in emission power is found at $Q = 17$, before dropping due to increased feedback of the THz mode on the indirect exciton. The inset shows the number of THz photons as a function of time for $Q = 1000$. For such a high quality factor the number of THz photons is considerably large. The resulting feedback on the excitonic modes is so strong it does not allow for a steady state solution. Rather, the number of THz photons oscillates, with a period in the range of 200 ps, mimicking the output of a Q-switched THz laser.

The energy diagram and stability curve of the system are shown in Figure 2. We used the following values of the parameters. The QW_1 material is $In_{0.1}Ga_{0.9}As$, the QW_2 is grown from $In_{0.08}Ga_{0.92}As$, and the spacer material is GaAs. The well widths are $d = 10$ nm, and the well separation 4 nm, with the tunneling rate set to $\hbar J = 6$ meV, which allows to estimate the effective electron hole separation as $L = 10$ nm. The optical Rabi splitting is $\hbar\Omega = 6$ meV and the tunable parameters are chosen as $\hbar\delta_\Omega = -3$ meV, and $\hbar\delta_J = 1$ meV. The eigenfrequency of the THz cavity was chosen as $\omega_T/2\pi = 1.74$ THz, and quality factor taken as $Q = 100$. The direct exciton scattering constant is estimated as $\alpha_1 = 6E_b a_B^2/S$, where $a_B = 10$ nm is the direct exciton Bohr radius, and $E_b = 8$ meV the binding energy. We take $S = 100\ \mu m^2$ as the system excitation area. The DX-IX interaction constant is taken from Ref. [6], and the indirect exciton scattering constant from the Ref. [8].

As one can see, parametrically instable solutions characterized by continuous THz emission exist over a wide region of pump intensity. The emission intensity depends on many parameters, including the quality factor Q of the THz cavity. This latter dependence is shown in Figure 3. One sees that there exists an optimal value of Q, which for the parameters we choose is about $Q = 17$. At small values of quality factor the dependence can be well approximated by Purcell formula.

AKNOWLEDGEMENTS

The presented results were obtained in collaboration with A.V. Kavokin (University of Southampton, UK). The work was supported by FP7 IRSES project "POLAPHEN" and AcRF Tier 1 project "Polaritonics for Novel Device Applications".

REFERENCES

1. K.V. Kavokin, M.A. Kaliteevski, R.A. Abram, A.V. Kavokin, S. Sharkova, I.A. Shelykh, *Appl. Phys. Lett.* **12**, 201111 (2010).
2. A.V. Kavokin, I.A. Shelykh, T. Taylor, M.M. Glazov, *Phys. Rev. Lett.* **108**, 197401 (2012).
3. T.C.H. Liew, M.M. Glazov, K.V. Kavokin, I.A. Shelykh, M.A. Kaliteevski, A.V. Kavokin, *Phys. Rev. Lett.* **110**, 047402 (2013).
4. P. Cristofolini, G. Christmann, S.I. Tsintzos, G. Deligeorgis, G. Konstantinidis, Z. Hatzopoulos, P.G. Savvidis, J.J. Baumberg, *Science* **336**, 704 (2012).
5. O. Kyriienko, A.V. Kavokin, I.A. Shelykh, *Phys. Rev. Lett.* **111**, 176401 (2012).
6. K. Kristinsson, O. Kyriienko, T.C.H. Liew, I.A. Shelykh, *Phys. Rev. B* **88**, 245303 (2013).
7. K. Kristinsson, O. Kyriienko, I.A. Shelykh, *Phys. Rev. A* **89**, 023836 (2014).
8. O. Kyriienko, E.B. Magnusson, I.A. Shelykh, *Phys. Rev. B* **86**, 115324 (2012).